BNL - 6/466
CAP-284-Muon-00C

MUON STORAGE RINGS - NEUTRINO FACTORIES

Zohreh Parsa
Brookhaven National Laboratory
Physics Department
Upton, New York

February 2000

Submitted to Proceedings of the Workshop on the "Next Generation Nucleon Decay and Neutrino Detector (NNN99)", SUNY, Stony Brook, NY, Sept. 23-25, 1999, AIP Press.

Muon Storage Rings- Neutrino Factories*

Z. Parsa

Brookhaven National Laboratory,
Physics Department 510A
Upton, New York 11973-5000, USA

E-mail: parsa@bnl.gov

February 2000

* Supported by U.S. Department of Energy Under Contract No. DE-AC02-98CH10886.
*Invited Paper; Submitted for Proceedings of the Workshop on the " Next generation Nucleon decay and Neutrino detector (NNN99)", SUNY, Stony Brook, September23-25, 1999, AIP-Press.

Muon Storage Rings - Neutrino Factories

Z. Parsa*

Brookhaven National Laboratory, Physics Department 510A, Upton, NY 11973-5000
E-mail: parsa@bnl.gov

Abstract. The concept of a muon storage ring based Neutrino Source (Neutrino Factory) has sparked considerable interest in the High Energy Physics community. Besides providing a first phase of a muon collider facility, it would generate more intense and well collimated neutrino beams than currently available. The BNL-AGS or some other proton driver would provide an intense proton beam that hits a target, produces pions that decay into muons. The muons must be cooled, accelerated and injected into a storage ring with a long straight section where they decay. The decays occurring in the straight sections of the ring would generate neutrino beams that could be directed to detectors located thousands of kilometers away, allowing studies of neutrino oscillations with precisions not currently accessible. For example, with the neutrino source at BNL, detectors at Soudan, Minnesota (1715 km), and Gran Sasso, Italy (6527 km) become very interesting possibilities. The feasibility of constructing and operating such a muon-storage-ring based Neutrino-Factory, including geotechnical questions related to building non-planar storage rings (e.g. at 8° angle for BNL-Soudan, and 31° angle for BNL-Gran Sasso) along with the design of the muon capture, cooling, acceleration, and storage ring for such a facility is being explored by our growing Neutrino Factory and Muon Collider Collaboration (NFMCC). We present overview of Neutrino Factory concept based on a muon storage ring, its components, physics opportunities, Possible upgrade to a full muon collider, latest simulations of front-end, and a new bowtie - muon storage ring design.

INTRODUCTION

Although many of the recent, exciting results in neutrino physics have been obtained by non-accelerator experiments, the neutrino mass and mixing parameters appear to require a new generation of accelerator based experiments. For this, an intense source of well-collimated neutrinos is needed.

Excitement is high in the accelerator physics community because atmospheric-neutrino results suggest that the long-baseline accelerator experiments such as MINOS [3], K2K [2], and NGS [4] should also find neutrino oscillations. Further, the LSND experiment that was conducted at a short-baseline accelerator facility, can be confirmed by future accelerator experiments such as MiniBooNE [5], ORLanD [6], and CERN P311 [7]. Moreover, physics associated with some interpretations of the solar-neutrino deficit may be accessible to studies in accelerator-based experiments, if neutrino-beam fluxes can be improved by 1-2 orders of magnitude.

To obtain a factor of 100 improvement in neutrino flux, the best prospect appears to be neutrino-beams derived from a muon-storage-ring, rather than from direct pion decays. However, such an approach requires considerable development before it can be realized in the laboratory. The idea of muon storage rings has been discussed since at least 1960 [8]. However, storage rings with enough circulating muons to provide higher intensity neutrinos than from conventional horn beams have only been considered more recently, in the context of muon collider technology [9].

The neutrino fluxes from the proposed muon-based beams would be higher than ever previously achieved with a much better-understood flavor composition. In addition, since the neutrino beams from these sources would be secondary beams from high energy muon decays, they would be extremely well collimated. Distances between production and detection could, therefore span the globe. Using the precisely known flavor composition of the beam, one could envision an extensive program to measure the neutrino oscillation mixing matrix, including possible CP violating effects.

A schematic concept of a Neutrino Factory Facility based on a muon storage ring, its components and physics opportunities are briefly discussed in section 2. A possible upgrade to a full muon collider is discussed in section 3. The examples described are based on some of the scenarios being explored by our Neutrino Factory and Muon Collider Collaboration (NFMCC),[10].

* Supported by US Department of Energy contract DE-AC02-98CH10886

NEUTRINO FACTORY

A neutrino factory based on a muon storage ring is a challenging extension of present accelerator technology. Conventionally, neutrino beams employ a proton beam on a target to generate pions, which are focused and allowed to decay into neutrinos and, muons [3]. The muons are stopped in the shielding, while the muon-neutrinos are directed toward the detector. In a neutrino factory, pions are made the same way and allowed to decay, but it is the decay muons that are captured and used. The initial neutrinos from pion decay are discarded, or used in a parasitic low-energy neutrino experiment. But the muons are accelerated and allowed to decay in a storage ring with long straight sections. It is the neutrinos from the decaying muons (both muon-neutrinos and anti-electron-neutrinos) that are directed to a detector.

Components

In a Neutrino Factory, a proton driver of moderate energy (< 50 GeV) and high average power,(e.g., 1-4 MW, similar to that required for a muon collider, but with a less stringent requirements on the charge per bunch and power is needed. This is followed by a target and a pion-muons capture system. A longitudinal phase rotation is performed to reduce the muon energy spread at the expense of spreading it out over a longer time interval. The phase rotation system may be designed to correlate the muon polarization with time, allowing control of the relative intensity of muon and anti-electron neutrinos. Some cooling may be needed, to reduce phase space, about a factor of 50 in six dimensions. This is much smaller than the factor of 10^6 needed for a muon collider. Production is followed by fast muon acceleration to 50 GeV (for example), in a system of linac and two recirculating linear accelerators (RLA's), which may be identical to that for a first stage of muon collider such as a Higgs Factory. A muon-storage ring with long straight sections could point to one or more distant neutrino detectors for oscillation studies, and to one or more near detectors for high intensity scattering studies.

Figure 1 illustrates components of a Neutrino Factory based on a racetrack - shaped muon storage lattice [10]. Alternately a planar bowtie - shaped ring can be designed and oriented to send neutrino beams to any two detector sites. Since,there is no net bending, the polarization may be preserved. (A disadvantage of the Bowtie - shaped ring is that it may need extra bending. Since there is geometry constrains on the ratio of short to long straight sections, the ring circumference may increase.) With the ring in a tilted plane, both long straight sections would point down into the earth, such that neutrinos can be directed

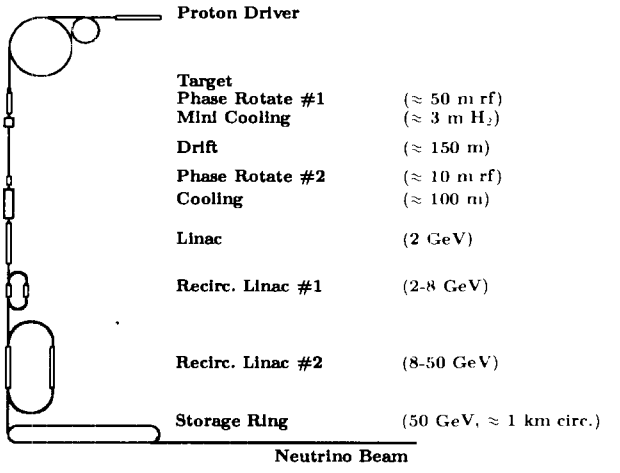

FIGURE 1. Overview of a Neutrino Factory Concept, with a Racetrack Muon - Storage Ring

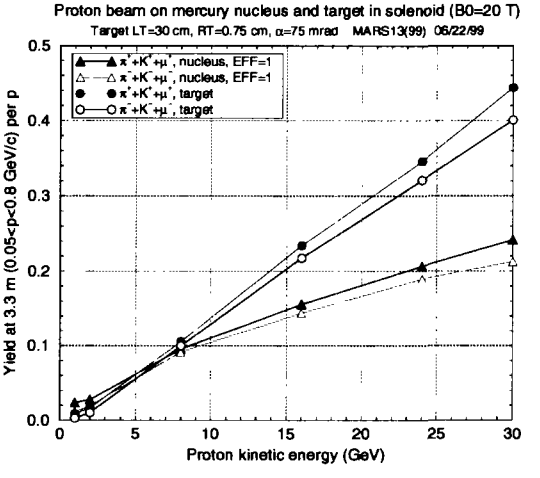

FIGURE 2. The number of pions produced per proton incident on a mercury target vs. proton energy. The yield at the target is shown by the circles, and the yield 3 m downstream of the target in a solenoid capture system is shown by the triangles.

into two very distant detectors. Triangular-shaped storage rings also have this advantage. In the following sections, a description of the targets, a simulation of target through cooling-channel and a new example of a bowetie-shaped muon storage lattice will be discussed.

Driver

The number of pions per proton produced with an optimized system varies linearly with the proton energy, as shown in Fig. 2. Thus, the number of pions, and the number of muons into which they decay, is essentially proportional to the proton beam power. The total six-

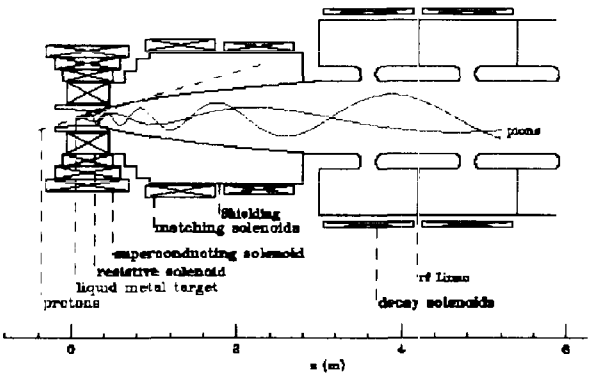

FIGURE 3. A Schematic of Targetry, Pion Capture, and beginning of Phase Rotation.

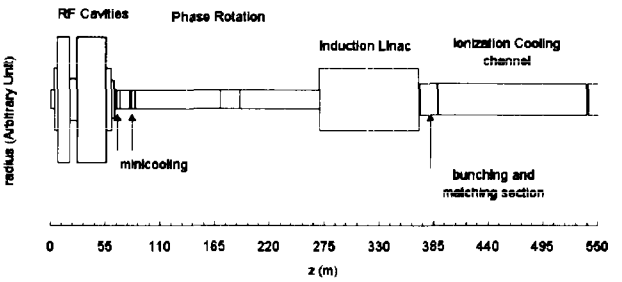

FIGURE 4. Schematics of the Muon Source from Target to Linac.

dimensional emittance of the produced muons depends on, e.g., the pion bunch length, and thus on the rms proton bunch length σ_p if that length is longer than the characteristic decay process length $c\,\tau^{\rm decay}$:

$$\tau^{\rm decay} = \frac{1}{\gamma_\pi^2}\,\frac{(m_\pi - m_\mu)}{m_\pi}\,\tau_\pi, \qquad (1)$$

where τ_π is the pion lifetime and $\gamma_\pi m_\pi$ is the pion energy. The pion yield peaks at $E_\pi \approx 300$ MeV, with $\tau^{\rm decay} \approx 1$ nsec. If the proton energy is low, this may imply a large tune shift:

$$\Delta\nu \propto \frac{n_p\, C}{\gamma_p^2\, \sigma_t\, \varepsilon_{transverse}} \propto \frac{n_p}{\gamma_p \langle B\rangle \sigma_t\, \varepsilon_{transverse}} \qquad (2)$$

in the proton ring before extraction, where C is the circumference of the proton driver, $\langle B\rangle$ is the average bending field, and $\varepsilon_{transverse}$ is the transverse emittance of the protons. The above dependency favors a higher proton energy. The total six-dimensional emittance of the produced pions depends also on the number of proton bunches employed to fill the storage ring. This favors a smaller number of large proton bunches in the driver, and thus a larger tune shift. Table 1 presents possible parameters for proton drivers at BNL and FNAL. The target requirements are very similar to those for the muon collider, except the instantaneous shock heating is somewhat less because protons are distributed in a larger number of bunches. In the scheme presented here, it is assumed that the liquid mercury jet solution is used. The capture solenoid is likely to be the same as described in the muon collider status report [9]. Figure 3, shows the pion production target, solenoidal capture, decay channel and beginning of phase rotation. At the end of this first phase rotation stage, the bunch length increases by about a factor of 6 and the energy spread decreases by the same amount. Whether this first stage of phase rotation can be eliminated is being investigated.

Target - Cooling Section

In this section a new integrated design for the Neutrino Factory front-end subsystem is described. Other designs and simulations are being explored by NFMCC. In the latest muon cooling simulation all the available subsystem simulations such as the target, pion capture and decay, phase rotation, matching, bunching and cooling were integrated together in such a way that the same particles generated at the target travels all the way to the end of the cooling channel. In this example [15], 16 GeV protons hits a carbon target, generates pions which then decay to muons. Figs. 4, Figs. 5 – Figs. 13, respectively, show schematics of Target to Linac Muon channel. (RF cavities are used for the 1st phase rotation and the Induction Linac for the second phase rotation). In addition the longitudinal and transverse phase distribution plots, at z=0 (target), z=370m (just before bunching), z=388m (just after bunching), and z=605m (after cooling) are shown. Particle composition in the target-to-linac channel is shown in Fig. 14, and in table 2. The muon emittance variation in the target-to-linac channel is shown in Fig. 15.

Cooling and Acceleration

The challenges of further acceleration and storage of the muon beam will be substantially easier if we reduce the transverse phase area of the beam by an additional factor of 10. This may not be accomplished in a single step of ionization cooling, but involves alternating ionization cooling and rf acceleration, all in a magnetic channel. The acceleration from $\sim$ 100 MeV to e.g., $\sim$ 50 GeV is best accomplished in recirculating linacs with superconducting rf cavities, after which muons are injected into a muon storage ring. The desire for multiply directed neutrino beams with very small angular divergence may require a more novel design for the storage ring, with a plane that is far from horizontal. The R&D needs for a muon collider are very similar, but with additional challenges in cooling and storage ring design. At least four

Table 1. Example of parameters for various Proton driver scenarios at BNL and FNAL.

	BNL_1	BNL_2	$FNAL_1$	$FNAL_2$
Energy [GeV]	24	24	16	16
Power [MW]	1	4	1	4
Rep. Rate [Hz]	2.5	5	15	15
p's/fill	10^{14}	$2\ 10^{14}$	$2.5\ 10^{13}$	10^{14}
Bunches	6	6	4	4
Circumference [m]	807	807	474	474
Bunch spacing [m]	135	135	118	118
σ_t [nsec]	1	1	1	1

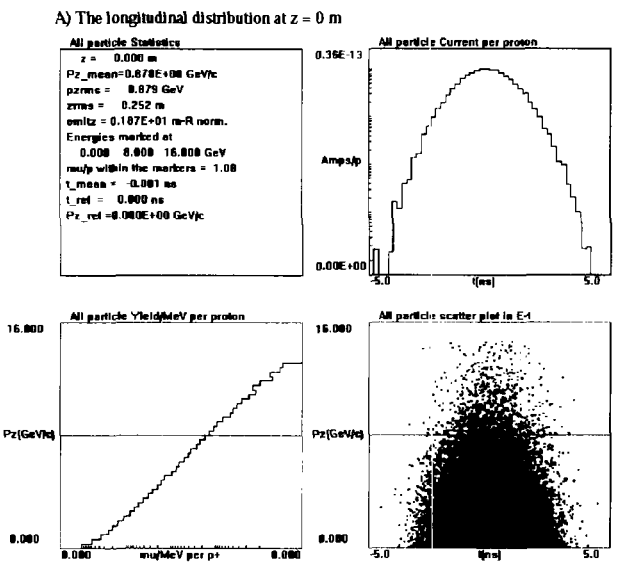

FIGURE 5. Longitudinal Phase distributions at z=0 (target). The scatter plot shows the distribution in P_z[GeV/c] vs t[ns], and the graphs above and to the left show the projection on to time and P_z axis.

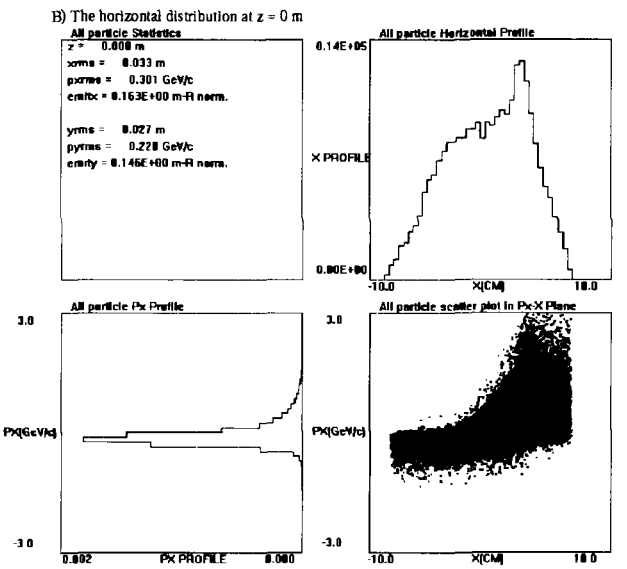

FIGURE 6. Horizontal Phase distributions at z=0 (target). The scatter plot shows the distribution in P_x[GeV/c] vs x[m] and the graphs above and to the left show the projection on to x and P_x axis.

orders of magnitude more cooling (including continual exchange between transverse and longitudinal emittance) are required for a muon collider than a neutrino factory. Also, a different ring is needed to maximize collider luminosity than simply to hold the muons while they decay.

Figure 16 shows a schematic of Ionization Cooling concept. Ionization cooling that has been proposed involves passing the beam through an absorber in which the muons lose transverse- and longitudinal-momentum by ionization loss (dE/dx). The longitudinal momentum is then restored by coherent re-acceleration, leaving a net loss of transverse momentum (transverse cooling). The process is repeated many times to achieve a large cooling factor. The beam energy spread can also be reduced using ionization cooling by introducing a transverse variation in the absorber density or thickness (e.g. a wedge) at a location where there is dispersion (the transverse position is energy dependent). Theoretical studies have shown that, assuming realistic parameters for the cooling hardware, ionization cooling can be expected to reduce the phase-space volume occupied by the initial muon beam by a factor of $10^5 - 10^6$. Ionization cooling is a new technique that has not yet been demonstrated. Special hardware needs to be developed to perform transverse and longitudinal cooling. It is recognized that understanding the feasibility of constructing an ionization cooling channel that can cool the initial muon beams by factors of $10^5 - 10^6$ is on the critical path to the overall feasibility of the

Table 2. Partice composition at various locations from Target to Linac, (with 16 GeV proton).

location	Z[m]	e^+/p^+	μ^+/p^+	π^+/p^+	k/p^+	p^+	total/p^+
Just after target	0	0.000	0.000	1.000	0.000	0.000	1.000
Just before minicooling	62	0.009	0.407	0.057	0.000	0.000	0.472
Just after minicooling	80	0.003	0.334	0.031	0.000	0.000	0.367
Just before bunching	370	0.039	0.265	0.001	0.000	0.000	0.305
Just after bunching	388	0.000	0.222	0.001	0.000	0.000	0.224
After cooling	605	0.000	0.101	0.000	0.000	0.000	0.101

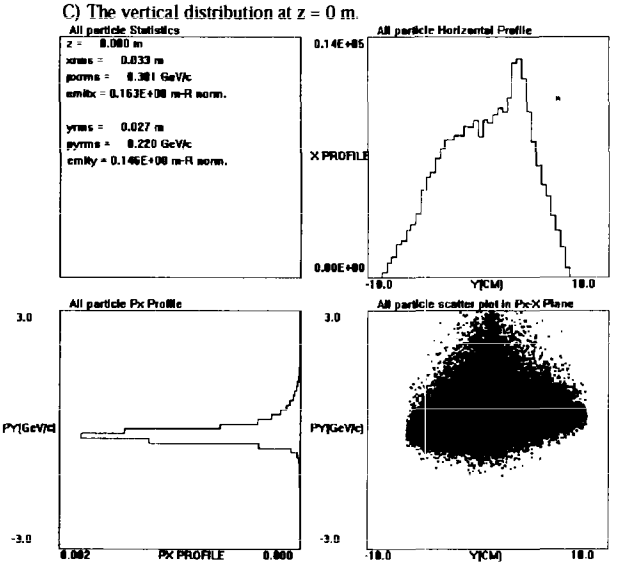

FIGURE 7. Vertical Phase distributions at z=0. The scatter plot shows the distribution in P_y[GeV/c] vs y[m] and the graphs above and to the left show the projection on to y and P_y axis.

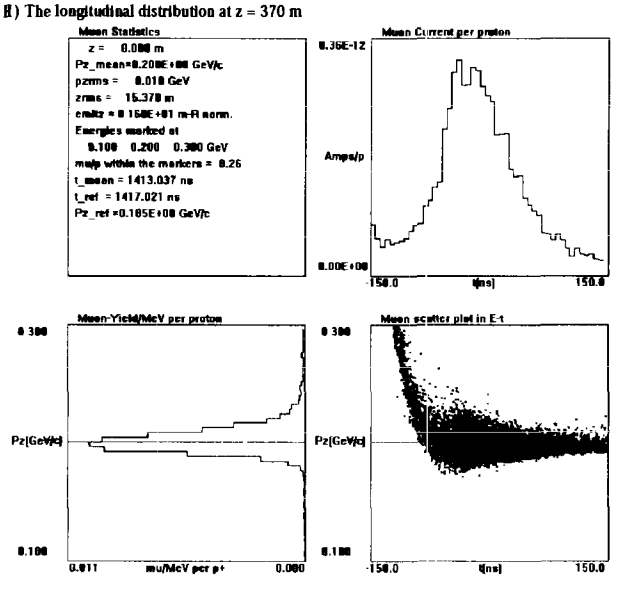

FIGURE 8. Longitudinal Phase distributions, same as Fig. 5 but for z= 370 m (just before bunching).

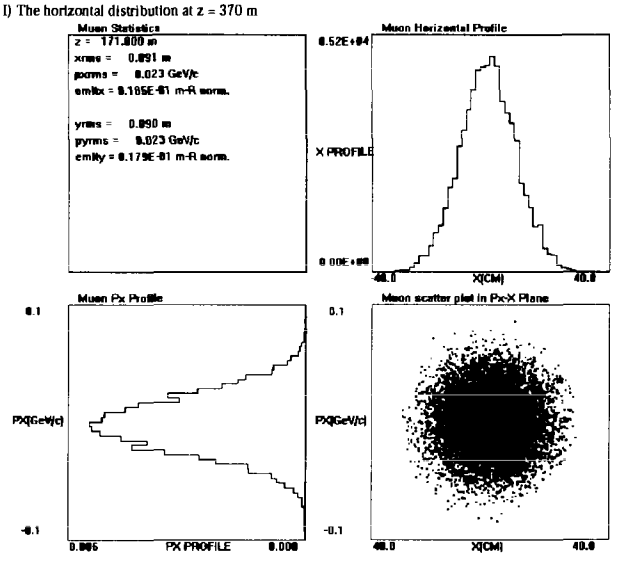

FIGURE 9. Horizontal Phase distributions, same as Fig. 6 but for z= 370 m (just before bunching).

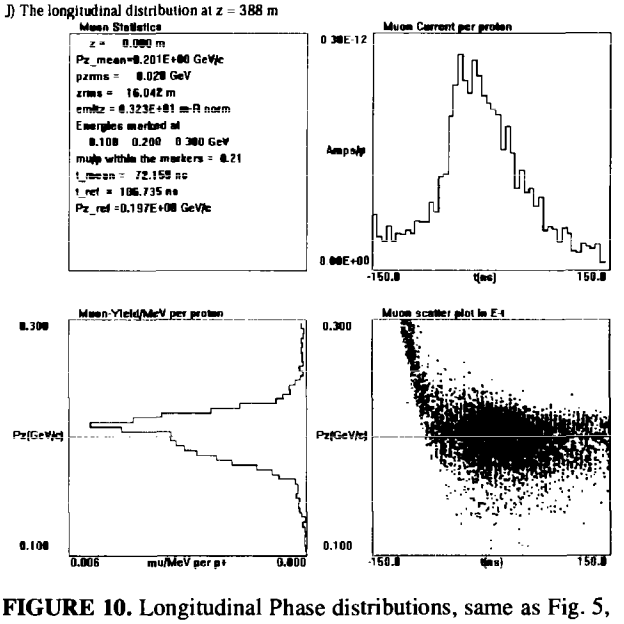

FIGURE 10. Longitudinal Phase distributions, same as Fig. 5, but for z= 388 m (just after bunching).

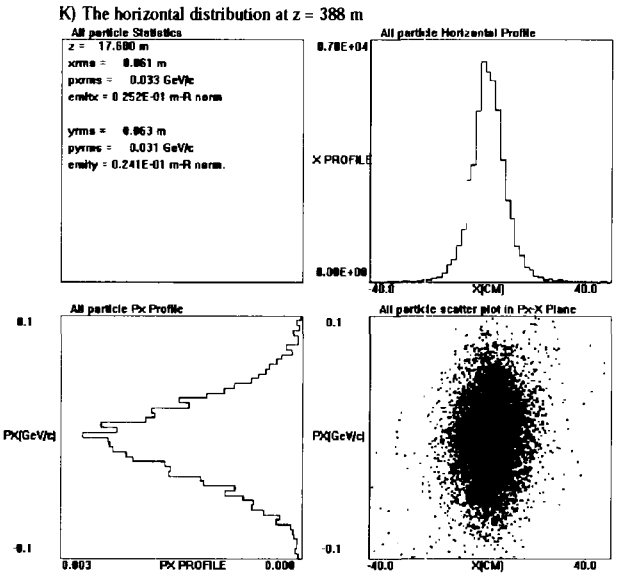

FIGURE 11. Horizontal Phase distributions, same as Fig. 6, but for z= 388 m (just after bunching).

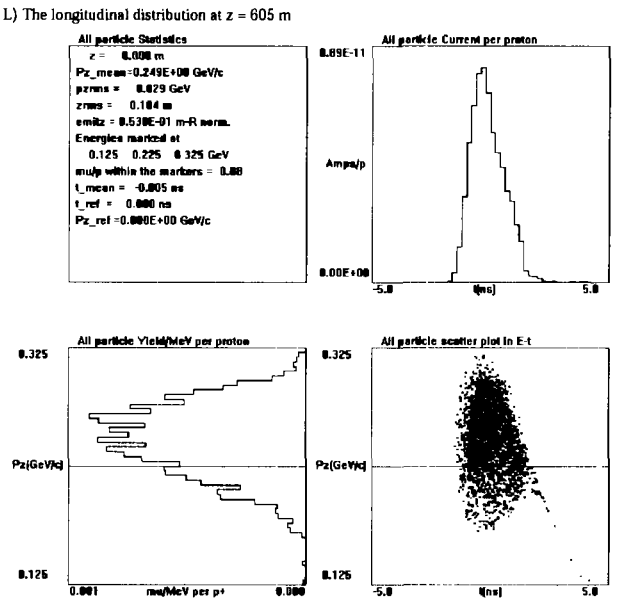

FIGURE 12. Longitudinal Phase distributions, same as Fig. 5, but for z= 605 m (after cooling).

muon collider concept. In Fig. 17, a schematic of the emittance exchange is shown.

Muon Storage Ring

A muon collider requires as its starting point, a very intense beam of muons with a small momentum spread. Such beams would be accelerated to collider energies and be used to search for new short distance high energy

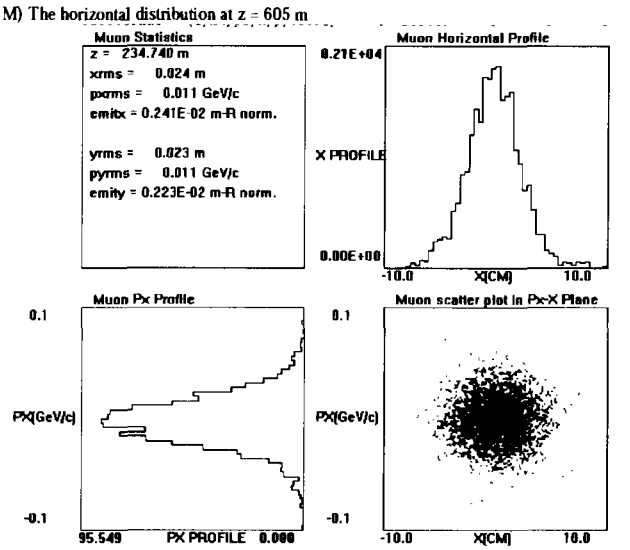

FIGURE 13. Horizontal Phase distributions, same as Fig. 6, but for z= 605 m (after cooling).

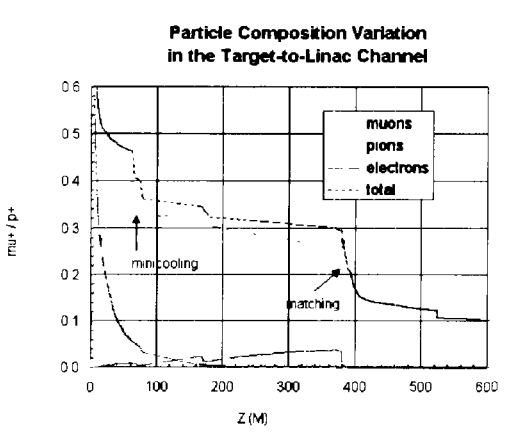

FIGURE 14. Particle Composition from Target to Linac.

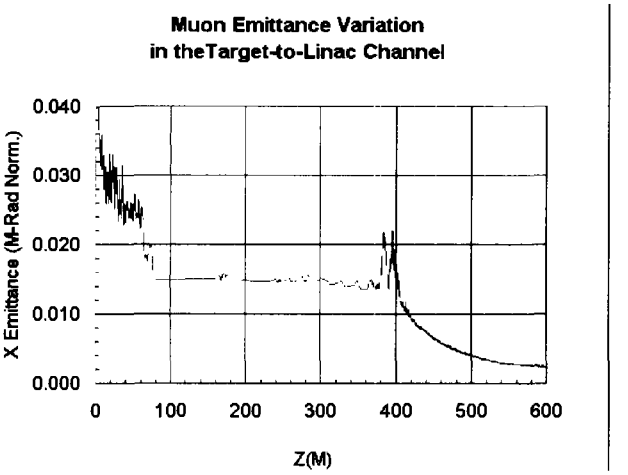

FIGURE 15. Muon emittance variation in Target to Linac channel.

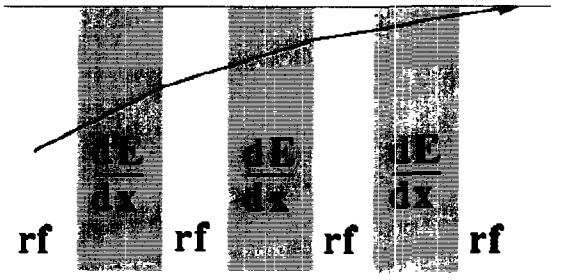

FIGURE 16. Schematic of Ionization Cooling concept (Ionization takes away momentum, and the RF acceleration puts momentum back along the z-axis, resulting in a Transverse Cooling).

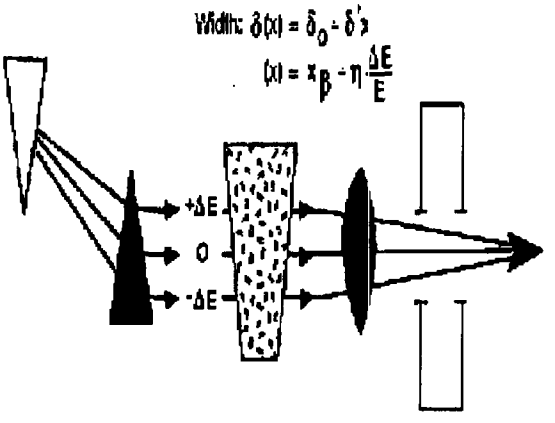

FIGURE 17. Schematic of the emittance exchange concept.

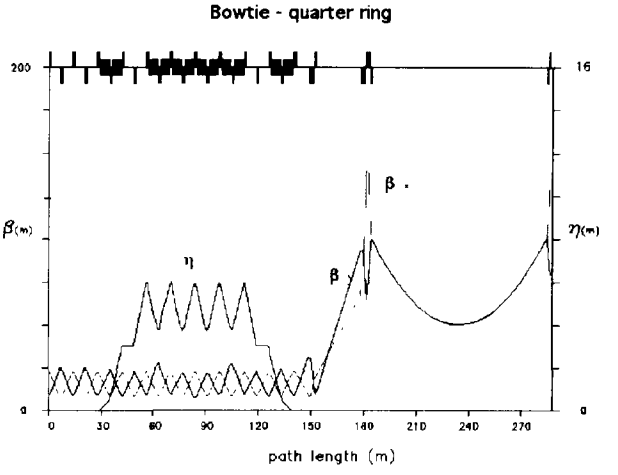

FIGURE 18. One Quarter of Bowtie MuonStorage Ring.

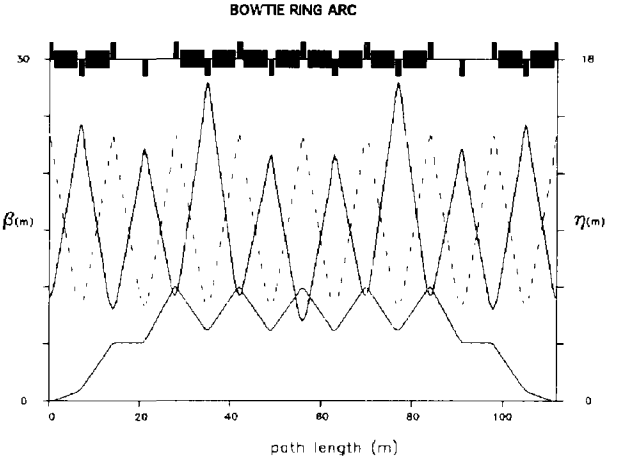

FIGURE 19. Bowtie-shaped Arc Lattice Functions.

phenomena. A neutrino factory based on a muon storage ring is a natural path to muon collider technology, since both facilities share essentially the same subcomponents prior to the storage ring. In previous sections we discussed some advantages and disadvantages of various shaped muon storage rings. Fig. 1 illustrated a racetrack - shaped configuration, with two long straight sections.

In this section a bowtie-shaped ring with a bypass is discussed. The planar ring can be designed and oriented to send neutrino beams to any two detector directions and with bypass(es) that could be added, to send beams to additional detector sites. In the bowtie-shaped lattice design [16], the lattice has two long-straight sections, two short-straight sections and two arcs. The description shown in Figs. 18 - 21 follows one quarter of the ring, starting at the center of the short straight section on the left side of the figure, and ends at the crossing point at the center of the bowtie. Table3 gives the parameters of the bowtie shaped ring. [Note, parameter optimizaton and additional lattice designs and simulations are being explored by NFMCC]. The short straight sections may be used for injection, and for RF. Half of the short straight section consists of two 14m arc cells without dipoles, and can be configured to provide (20m) free space for injection.

Each arc contains eight FODO cells, two without dipoles. There are 60 deg cell phase advances, and the dipole-free cells act as dispersion suppressors. Twelve 5m long dipoles each bend the beam by 10 deg, so the arc has 120 deg of bending. This amount of bending causes the long beam-lines to intersect at 60 deg (a typical angle, whose exact value depends on the selection of ring and detector sites). The long dispersion-free straight section provides a muon beam such that the decaying muons generate low divergence neutrinos. Two different configurations are shown in Fig. 20 and Fig. 21. In one, the long straight section has quadruples in the center (around the crossing point) making two beam waists, each with 50m

Table 3. Lattice Parameters for a Bowtie - Shaped Muon Storage Ring.

Energy	50 GeV
Circumference	1150 m
$L_{shortstraightsections}$	20 m
$L_{oflongstraightsections}$	200 m
Dipole field	5.82 T
$Gradient_{Maximum}$	30 T/m
Dipole length	5 m
Arc cell length	14 m
Cell phase advance	60 deg
Ring tunes	9.85, 9.23
$Betafunction_{Maxima}$:	
Arc	28 m
Long straight sections	100 m
Ring	151 m
Dispersion:	
Maximum	6 m
Minimum	-6 m
Momentum compaction	0.025
Chromaticity:	
Horizontal	12.5
Vertical	11.5
Beam crossing angle	60 deg

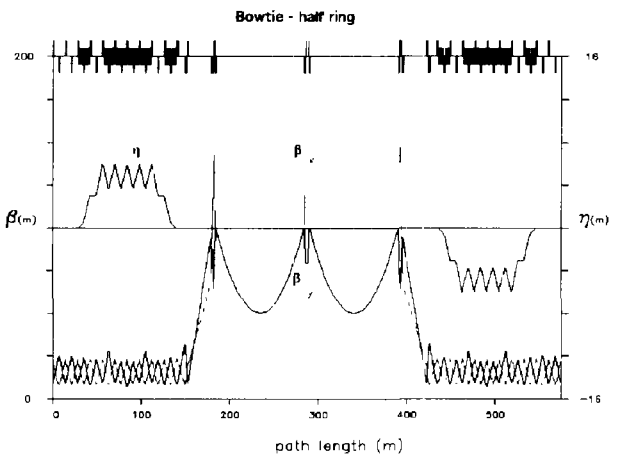

FIGURE 20. Lattice Functions for Bowtie-shaped Half Ring.

beta function values. In the other configuration, a 200-meter magnet-free beam-line is provided, with a beam waist at the center with 100 m beta values.

A racetrack muon storage - ring can be configured to deliver one neutrino beam to an arbitrary detector site. Bowtie - shaped, triangle shaped rings can be configured to deliver neutrino beams to two arbitrarily selected detector sites. This can be done by appropriate choice of, 1) the ring plane, 2) the orientation of the ring in that plane

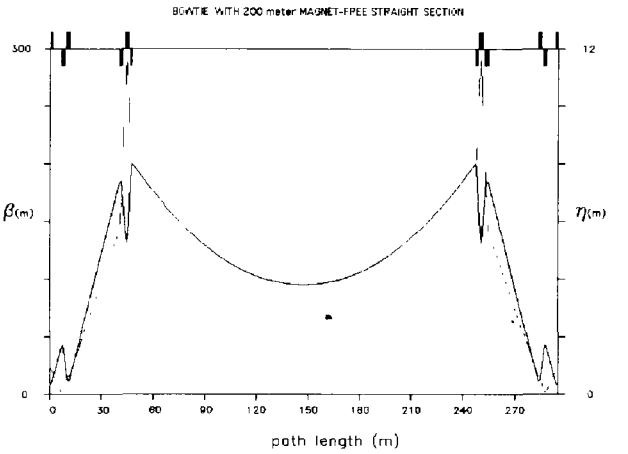

FIGURE 21. Lattice functions for Bowtie-shaped - Long Straight Section Alternative Configuration.

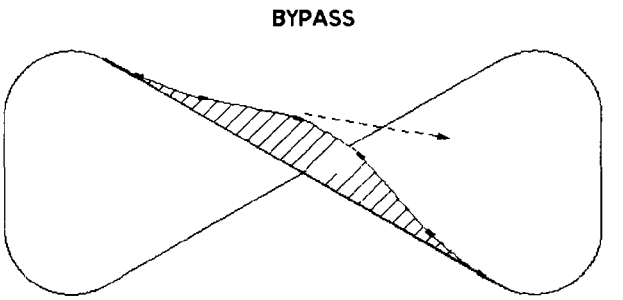

FIGURE 22. Lattice functions for Bowtie-shaped Ring with Bypass. The arrow illustrates direction of a neutrino beam to additional detector site(s) via the Bypass.

and 3) the angle at the crossing point between the two long straight sections. By inclusion of bypasses, additional detector sites may be accessible from a single muon storage-ring source.

A bypass would lie in a plane that includes the original long straight section (but differs from that of the ring), and begin and end on one of the long straight sections. Its magnets would be powered when one desires to send the muons along the deformed bypass path rather than along the normal straight path. In such a bypass, dipoles would produce a roughly triangular path in the bypass plane, one of whose sides would point to the desired detector. The two necessary degrees of freedom are provided by the angle between the bypass and ring planes and by the magnitude of the deflection given by the bypass dipoles. To suppress the dispersion pairs of dipoles should be placed 180 deg apart, in FODO cells.

A Schematic of Neutrino Factory concept, with a bowtie-shaped muon storage ring is illustrated in Fig. 23. The geometry of the storage ring depends on locations of the ring and detector . Table 5 shows direct distances

Table 4. The numbers of surviving muons after various stages in the accelerator complex.

P driver energy	Factor	24[GeV] μ/p	16 [GeV] μ/p
Pions After: Match*		0.66	0.44
1st Phase Rotation	0.45	0.3	.2
2nd Phase Rotation	0.7	0.21	.14
RF Capture	0.7	0.15	.1
Cooling	0.9	0.13	.09
Acceleration	0.7	0.092	.061
$n_\mu/(n_p\, E_p)$ [GeV^{-1}]		.0038	.0038

* (< 1 GeV, forward)

from rings at BNL or FNAL to Gran Sasso, Soudan and SLAC.

Physics Potentials - Event Rates

A neutrino factory has a strong independent physics case. It would be easier to build, less expensive than a full muon collider, and could demonstrate most of the components of a collider. For the example of Neutrino Factory Facility based on a muon storage ring (Fig. 1), the number of surviving muons, per incident proton, at various stages of the accelerator complex are summarized in Table 4, [10].

The number of neutrino interactions per unit mass of a detector at distance L from a muon storage ring operating at energy E_μ scales as

$$N_{\text{events}} \propto N_\mu\, E_\mu^3\, L^{-2}. \tag{3}$$

Table 4 illustrates the muon survival efficiencies, for the example of a proton source with 1.5 MW power, in one year (10^7 s) of operation, there would be about 4×10^{20} muons per year decaying in the storage ring. Assuming the fraction of the ring pointing to a given detector to be about 0.25 (as in example of a bowtie-shaped muon storage) then the number of decays pointing to the given detector will be approximately 10^{20}. It may be noted that the number of events with the 1.5 MW neutrino factory, in a detector at the same 730 km, is approximately 100 times that in the proposed CERN - Gran Sasso experiment (NGS [4]), and about 40 times the maximum event rate that MINOS [3] can expect. Upgrading the proton driver to 4 MW, the factors become about 300 and 100 for Gran Sasso and Soudan, respectively.

Table 5 gives charged current neutrino interaction rates (per kiloton-year) as a function of baseline length L for an $E_\mu = 50$ GeV muon storage ring in which there are 1×10^{20} unpolarized muon decays per year within a neutrino beam-forming straight section [17]. The rates are listed for oscillations:

1) $\nu_e \to \nu_\mu$: $\Delta m^2 = 3.5 \times 10^{-3}$ eV^2/c^4 & $\sin^2 2\theta = 0.1$,

2) $\nu_e \to \nu_\mu$: $\Delta m^2 = 1 \times 10^{-4}$ eV^2/c^4 & $\sin^2 2\theta = 1$,

3) $\nu_e \to \nu_\tau$: $\Delta m^2 = 3.5 \times 10^{-3}$ eV^2/c^4 & $\sin^2 2\theta = 0.1$,

4) $\nu_\mu \to \nu_\tau$: $\Delta m^2 = 3.5 \times 10^{-3}$ eV^2/c^4 & $\sin^2 2\theta = 1$.

The rates for the unoscillated neutrino interactions, the corresponding statistical significance of the disappearance signal (numbers in parenthesis), and the rates for the antineutrino interactions, are also included in Table 5

.

Neutrino Oscillation

With only two massive neutrinos, with mass difference $\Delta m^2 = m_2^2 - m_1^2$, mass eigenstates ν_1 and ν_2 with mixing angle θ, the flavor eigenstates become:

$$\begin{pmatrix} \nu_a \\ \nu_b \end{pmatrix} = \begin{pmatrix} \cos\theta & \sin\theta \\ -\sin\theta & \cos\theta \end{pmatrix} \begin{pmatrix} \nu_1 \\ \nu_2 \end{pmatrix}. \tag{4}$$

The probability that a neutrino of flavor ν_a and energy E appears as flavor ν_b after traversing distance L in vacuum is

$$P(\nu_a \to \nu_b) = \sin^2\left(1.27\Delta m^2[\text{eV}^2]\frac{L[\text{km}]}{E[\text{GeV}]}\right)\sin^2 2\theta. \tag{5}$$

Since the atmospheric neutrino data involves GeV muon neutrinos with distance scales of the Earth's diameter, this suggests Δm^2 of order 10^{-3} (eV)^2 for $\sin^2 2\theta \approx 1$. The solar neutrino data involves MeV electron neutrinos and distance scales of the radius of the Earth's orbit, suggesting Δm^2 of order 10^{-10} (eV)^2 with $\sin^2 2\theta \approx 1$ for vacuum oscillations [18]. The LSND result involves 30-MeV muon antineutrino and a distance scale of 30 m, suggesting Δm^2 of order 1 (eV)^2; large mixing angles are excluded by reactor data [19], thus, $\sin^2 2\theta$ can only be of order 10^{-2} in this case. Obviously, four different massive neutrinos are required to accommodate all three results, given their disparate scales of Δm^2. The Standard Model presently includes only three neutrinos with standard electroweak couplings and $m_\nu < m_Z/2$, so a "sterile" neutrino is required if all the data are correct [20]. Even discarding the LSND result, three massive neutrinos are required with a corresponding 3×3 mixing matrix, e.g.

$$\begin{pmatrix} \nu_e \\ \nu_\mu \\ \nu_\tau \end{pmatrix} = \begin{pmatrix} c_{12}c_{13} & s_{12}c_{13} & s_{13}e^{-i\delta} \\ -s_{12}c_{23} - c_{12}s_{13}s_{23}e^{i\delta} & c_{12}c_{23} - s_{12}s_{13}s_{23}e^{i\delta} & c_{13}s_{23} \\ s_{12}s_{23} - c_{12}s_{13}c_{23}e^{i\delta} & -c_{12}s_{23} - s_{12}s_{13}c_{23}e^{i\delta} & c_{13}c_{23} \end{pmatrix} \begin{pmatrix} \nu_1 \\ \nu_2 \\ \nu_3 \end{pmatrix} \tag{6}$$

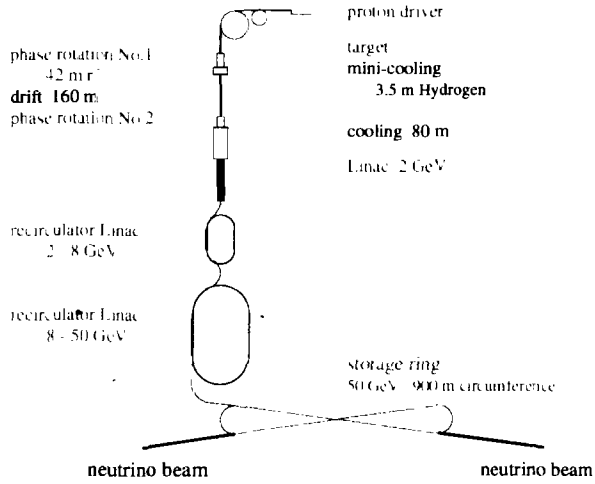

FIGURE 23. Neutrino Factory Concepts, with a Bowtie-Shaped Muon Storage Lattice.

a MNS matrix [21], where $c_{12} = \cos\theta_{12}$, *etc.*., In the three massive neutrino model, the neutrino oscillation probabilities of interest depends on six measurable parameters: three mixing angles (θ_{12}, θ_{13}, θ_{23}); a phase δ related to CP violation as indicated in eq. (6); and two differences of the squares of the neutrino masses (Δm^2_{12} and Δm^2_{23} for instance). The interpretation of the solar and atmospheric neutrino data in terms of the three-neutrino oscillation hypothesis suggests $|\Delta m^2_{12}| \ll |\Delta m^2_{23}|$, with Δm^2_{12} and Δm^2_{23} being responsible for the transitions and/or oscillations of the solar and atmospheric neutrinos, respectively.

The description of the atmospheric neutrino data requires $\Delta m^2_{23} \approx (2-6) \times 10^{-3}$ eV^2 and large mixing angle θ_{23}: $\sin^2 2\theta_{23} \approx (0.9-1.0)$. For $|\Delta m^2_{12}| \ll |\Delta m^2_{23}|$ and with Δm^2_{23} in the above range, the non-observation of oscillations of the reactor electron antineutrinos in the CHOOZ experiment [22] implies a limit on the angle θ_{13}: $\sin^2\theta_{13} < 0.11$. Given these constraints, the transitions/oscillations of the solar neutrinos in the three-neutrino mixing scheme under discussion depend largely on the remaining two parameters: Δm^2_{12} and $\sin^2 2\theta_{12}$.

Further, the presence of matter may modify the oscillations of electron neutrinos because of their charged-current interaction (MSW effect [23]). In particular, the oscillations can be resonantly enhanced by the matter effects even when the oscillation probabilities are small in vacuum. This leads to additional interpretations of the solar neutrino data in which Δm^2_{12} can be of order 10^{-5} (eV)^2 [24]. In effect at the present time , there are four viable interpretations of the solar neutrino data:

1) Vacuum oscillation (VO) solution with $\Delta m^2_{12} \approx (0.5-5.0) \times 10^{-10}$ eV^2 and $\sin^2 2\theta_{12} \approx (0.7-1.0)$,

2) Low MSW solution corresponding to $\Delta m^2_{12} \approx (0.5-2.0) \times 10^{-7}$ eV^2 and $\sin^2 2\theta_{12} \approx (0.9-1.0)$,

3) Small mixing angle (SMA) MSW solution with $\Delta m^2_{12} \approx (4.0-9.0) \times 10^{-6}$ eV^2 and $\sin^2 2\theta_{12} \approx (0.001-0.01)$,

4) Large mixing angle (LMA) MSW solution, $\Delta m^2_{12} \approx (0.2-2.0) \times 10^{-4}$ eV^2 and $\sin^2\theta_{12} \approx (0.65-0.96)$.

With four interpretations of the solar neutrino data, and the two interpretations of the LSND data as either right or wrong, there are a total of eight scenarios for explanations of the data. The experimental challenge is to reduce these to a single scenario, and to make accurate measurements of the parameters of that scenario.

Thus, with the available experimental guidelines as to the parameters of neutrino masses and mixings, one can begin to plan for more extensive studies namely, with neutrino beams derived from the decay of muons in a storage ring. Both μ^- and μ^+ can be stored in the ring, but only one sign would be used at a time. For example if μ^- are stored, their decay

$$\mu^- \rightarrow e^- \nu_\mu \overline{\nu}_e, \tag{7}$$

leads to beams with nearly equal numbers of ν_μ and $\overline{\nu}_e$ with spectra that are well known.

At the detectors, the neutrino and the antineutrino may or may not have changed their flavor, leading to the appearance of a different flavor or the disappearance of the initial flavor, respectively. When detected by a charged-current interaction, there are 6 classes of signatures in a three-neutrino model: 1) $\nu_\mu \rightarrow \nu_e \rightarrow e^-$ (appearance); 2) $\nu_\mu \rightarrow \nu_\mu \rightarrow \mu^-$ (disappearance); 3) $\nu_\mu \rightarrow \nu_\tau \rightarrow \tau^-$ (appearance); 4) $\overline{\nu}_e \rightarrow \overline{\nu}_e \rightarrow e^+$ (disappearance); 5) $\overline{\nu}_e \rightarrow \overline{\nu}_\mu \rightarrow \mu^+$ (appearance); 6) $\overline{\nu}_e \rightarrow \overline{\nu}_\tau \rightarrow \tau^+$ (appearance).

For operation with positive muons, a similar list of processes may be written. The 5th process where a muon

Table 5. Neutrino Interaction Rates at a Neutrino Factory.

		Source at Detector at L (km)	BNL G. Sasso 6528	BNL SLAC 4139	BNL Soudan 1712	FNAL G. Sasso 7332	FNAL SLAC 2899	FNAL Soudan 732
Case		Mode						
1)	μ^+	$\nu_e \to \nu_\mu$	90	160	190	63	180	200
		$\nu_e \to \nu_e$	1400	3600	16000	1100	8000	1.2×10^5
			(2.4σ)	(2.7σ)	(1.5σ)	(1.9σ)	(2.0σ)	(0.6σ)
		$\bar{\nu}_\mu \to \bar{\nu}_\mu$	890	2200	9300	700	4800	7.0×10^4
2)	μ^+	$\nu_e \to \nu_\mu$	5×10^{-2}	0.86	1.5	3×10^{-5}	1.3	1.6
		$\nu_e \to \nu_e$	1500	3800	16000	1200	8200	1.2×10^5
		$\bar{\nu}_\mu \to \bar{\nu}_\mu$	890	2200	9400	700	4800	7.0×10^4
3)	μ^+	$\nu_e \to \nu_\tau$	31	60	70	20	67	73
		$\nu_e \to \nu_e$	1400	3700	1.6×10^4	1100	8000	1.2×10^5
			(2.4σ)	(2.7σ)	(1.5σ)	(1.9σ)	(2.0σ)	(0.6σ)
		$\bar{\nu}_\mu \to \bar{\nu}_\mu$	890	2200	9400	700	4800	7.0×10^4
4)	μ^-	$\nu_\mu \to nu_\tau$	450	570	650	410	620	680
		$\nu_\mu \to \nu_\mu$	760	3100	1.7×10^4	490	8000	1.4×10^5
			(35σ)	(23σ)	(12σ)	(40σ)	(16σ)	(4.6σ)
		$\bar{\nu}_e \to \bar{\nu}_e$	770	1900	8100	600	4100	6.1×10^4

of different sign from the parent muon appears, has a very unique possibilities at a neutrino factory based on muon storage rings. Since they are the only sources of intense high energy electron (anti)neutrino beams. The τ appearance (cases 3 and 6) are practical only for neutrino beams with 10's of GeV energy.

It is anticipated that by the time a muon storage ring would be built the two angles (θ_{23} and θ_{12}), and the magnitudes of two mass squared differences (Δm^2_{23} and Δm^2_{12}) would be known, from the solar and atmospheric neutrino measurements (which would have been verified by long baseline and reactor experiments), for example, MINOS and KamLAND. The remaining pieces of the puzzle would be θ_{13}, the CP-violating phase δ and the signs of the Δm^2_{ij}. Moreover, the indicated long-baseline experiments will not be sensitive to the matter effects in neutrino oscillations because the distances between the sources and detectors are not sufficiently large. Verifying the existence of matter effects in neutrino oscillations by observing directly the modification of the neutrino oscillation probabilities by these effects, would also be fundamental and interesting.

The third mixing angle θ_{13} can be measured in several channels at a neutrino factory [25]. The detector must be far to avoid background but not too far (< 1000 km) so that the effects of Δm^2_{12} remain negligible and thus δ can formally be set to zero. Fig. 24 shows the achievable sensitivity to the yet-unknown value of θ_{13}.

Fig. 24 illustrates sensitivity reach in the

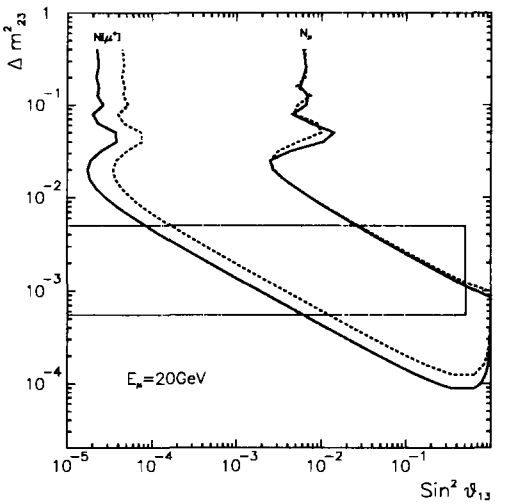

FIGURE 24. Sensitivity reach in the $(\sin^2\theta_{13}, \Delta m^2_{23})$ plane.

$(\sin^2\theta_{13}, \Delta m^2_{23})$ plane for a 10 kton detector and a neutrino beam from 2×10^{20} decays of 20 GeV muons in a storage ring at distance 732 km. The appearance process $\bar{\nu}_e \to \bar{\nu}_\mu \to \mu^+$, shown by the lines on the left, has much greater sensitivity than the disappearance process $\nu_\mu \to \nu_\mu \to \mu^-$, shown by the lines on the right. The interior of the box is the approximate region allowed by Super-Kamiokande data [25].

CP Violation

The three-neutrino scenario [26] can lead to CP violation in for example

$$A_{\rm CP} = \frac{P(\nu_e \to \nu_\mu) - P(\bar{\nu}_e \to \bar{\nu}_\mu)}{P(\nu_e \to \nu_\mu) + P(\bar{\nu}_e \to \bar{\nu}_\mu)}, \qquad (8)$$

or time-reversal violation

$$A_{\rm T} = \frac{P(\nu_e \to \nu_\mu) - P(\nu_\mu \to \nu_e)}{P(\nu_e \to \nu_\mu) + P(\nu_\mu \to \nu_e)}. \qquad (9)$$

The asymmetry (8) can be measured using wrong-sign muons and the two charges of the muon beam. However, the genuine CP violating contribution to (8) due to a non-vanishing phase δ competes with terms related to matter effects, *i.e.*, to the different rates of evolution for ν_e and $\bar{\nu}_e$ between source and detector. The relative strength of the matter-induced asymmetry increases quadratically with distance, and dilutes the signal of CP violation in a far detector.

If the solution to solar neutrino problem involves, large mixing angles and matter enhancement (LMA MSW, $\sin^2 2\theta_{12} \approx \sin^2 2\theta_{23} \approx 1$), then there is a possibility of measuring the CP violating asymmetry (8), with expression

$$|A_{\rm CP}| \approx \left| \frac{2\sin\delta}{\sin 2\theta_{13}} \sin\left(\frac{1.27\Delta m^2_{12} L}{E}\right) \right|, \qquad (10)$$

provided the detector is located sufficiently far and high statistics ($> 10^{21}$ muons per year) are available. For all the other solar neutrino solutions $A_{\rm CP}$ is extremely small, being suppressed by a factor of either $\sin^2 2\theta_{12}$ or Δm^2_{12}. Figure 25 Show the CP violating asymmetry (8) divided by statistical uncertainties *vs.* distance L for a 10 kton detector in a beam from 2×10^{21} muon decays. A large angle MSW scenario is supposed, with $\Delta m^2_{12} = 10^{-4}$ eV^2, $\Delta m^2_{23} = 2.8 \times 10^{-3}$ eV^2, $\theta_{12} = 22.5°$, $\theta_{13} = 13°$, $\theta_{23} = 45°$, and $\delta = -90°$ (corresponding to large CP violation). The dashed curves ignore matter effects, while the solid curves include them; the matter effects dominate the asymmetry for distances beyond 1000 km. The lower (upper) curves are for $E_\mu = 20$ (50) GeV, from [hep-ph/9909254].

The asymmetry (9) is not sensitive to matter effects, but relies on distinguishing the process $\nu_\mu \to \nu_e \to e^-$ from $\bar{\nu}_e \to \bar{\nu}_e \to e^+$. In the detector, it will be very difficult to distinguish electrons from positrons but the relative ν_μ and $\bar{\nu}_e$ fluxes can be varied by varying the polarization of the muons in the storage ring [27].

If future experiments confirm the interpretation of the LSND data that there exist more than three light neutrinos, then use of the neutrino factory flavor-rich beams would be even more crucial, because the parameter space for CP/T violating effects would be considerably enlarged and could be explored in experiments with such beams [28].

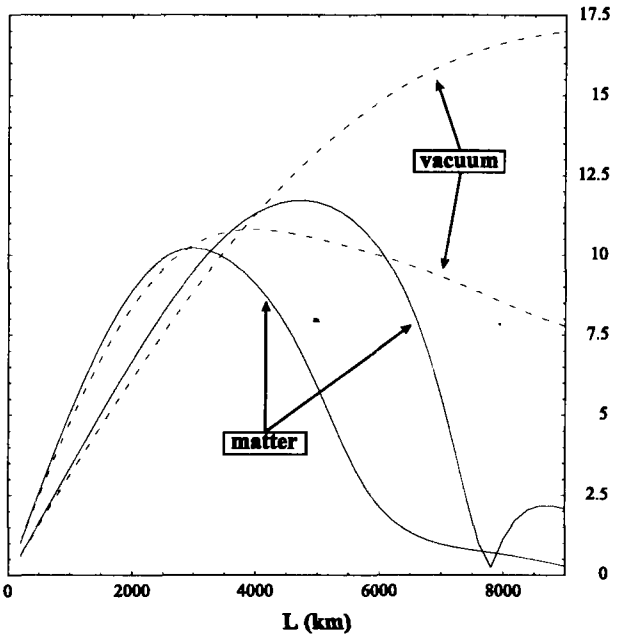

FIGURE 25. CP violation signal over statistical uncertainties versus distance.

Precision Physics

Muon storage ring based neutrino beams would bring about new neutrino oscillation measurements, and a new era for high-precision neutrino scattering experiments [29]. For example, with a detector located 30 m from a 150 m straight section of a 50-GeV, 10^{21}-μ/yr muon storage ring, the event rate is 40 million events per kilogram per year over a 10 cm radius. Oscillation-related measurements may be interpreted precision measurements of the total neutrino and antineutrino cross sections, as well as of the beam divergence. As precision probes of nuclear and nucleon structure, the neutrinos may be used to provide additional information to that obtained with charged lepton beams, in related studies. It is known that, neutrino scattering allows a clean separation of the valence and sea quark distributions, and use of a polarized target permits characterization of the spin dependence of these distributions. Thus, near detectors are the natural successor to nucleon structure measurements presently underway at HERA, HERMES, Jefferson Lab, RHIC and elsewhere. For example, scattering of the four neutrino types ν_μ, $\bar{\nu}_\mu$, ν_e, and $\bar{\nu}_e$ off electrons could lead to measurements of the Weinberg angle ten times better than known at present.

Note that, a high-flux multi-GeV neutrino beam is a charm factory, in which a ν_μ beam leads to c quarks

that are tagged by a final-state μ^- ($\nu_\mu d \to \mu^- c$), while $\bar{\nu}_\mu$ beam leads only to tagged $\bar{c}$ quarks. For example, for the above described beam parameters, there would be 10^7 leptonic tagged charm decays in only 40 kg-years (not kton-years!), permitting measurements of V_{cd} to fraction of a percent, and perhaps even direct observation of $D^0 - \overline{D}^0$ mixing.

MUON COLLIDER

A muon collider with center of mass energy less than about 10 TeV can be circular and relative to NLC (a Next Linear Collider) of the same energy, it could be far smaller in size. For the same luminosity a muon collider can tolerate a far larger spot size than an electron linear collider since the muons make about 1000 crossings. Since there is little beamstrahlung, very small energy spread is easily obtainable. Fig. 26 shows a schematic of a muon collider components [9]. A high intensity proton source is bunch compressed and focused on a heavy metal target. The pions generated are captured by a high field solenoid and transferred to a solenoidal decay channel within a low frequency linac. The linac reduces, by phase rotation the momentum spread of the pions and of the muons into which they decay.

Subsequently, the muons are cooled by a sequence of ionization cooling stages. Each stage consists of energy loss, acceleration, and emittance exchange by energy absorbing wedges in the presence of dispersion. Once they are cooled the muons must be rapidly accelerated to avoid decay losses. This can be done in recirculating accelerators (as at CEBAF) or in fast pulsed synchrotrons. Muon collisions occur in a separate high field collider storage ring with a single very low beta insertion.

It is expected that the first stage, proton driver would be 16 to 30 GeV; but would be much faster pulsed, keeping the number of protons per pulse the same or smaller than the AGS, which is about 6×10^{13} protons per pulse and with some upgrade to about 10^{14} protons per pulse.

Roughly one expect to get 1 muon/proton on target which would give luminosity between 10^{34} to 10^{35} the envisioned muon collider. Although the accelerating component is large, the other components can fit within it and the whole machine is compact enough to fit on existing Brookhaven or Fermilab sites.

For more information on the Muon Collider and parameters under study, see e.g. [9],[30] – [36]. Table 6 shows the parameters of potential muon colliders at 100 GeV, 500 GeV and 4 TeV center of mass energy. The 100 GeV collider would be ideal for the study of the lowest mass Higgs. The 4 TeV collider should be in the

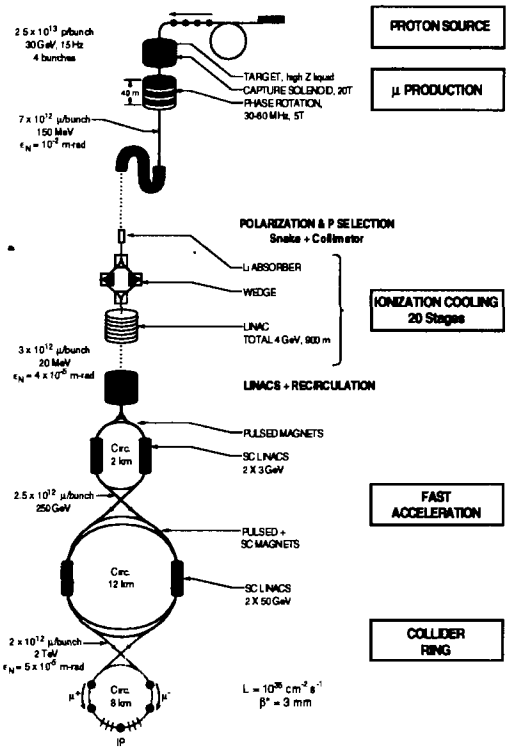

FIGURE 26. Schematic of a Muon Collider.

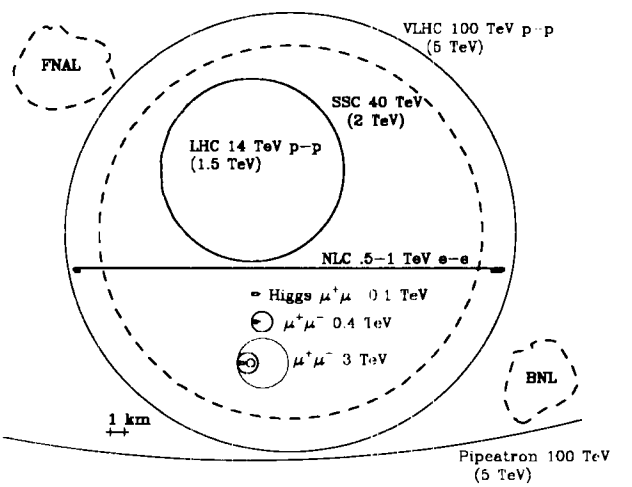

FIGURE 27. Comparison of relative sizes of Muon Collider, Large Hadron Collider (LHC), and Next Linear Collider (NLC), relative to the BNL and FNAL sites.

Table 6. Parameters of $\mu^+\mu^-$ collider Rings.

Energy (C.M.) TeV	4	0.5	0.1
Beam Energy TeV	2	0.25	0.05
Beam γ	19,000	2,400	473
Rep. rate Hz	15	2.5	15
p Energy GeV	30	24	16
p/pulse	10^{14}	10^{14}	5×10^{13}
μ/bunch	2×10^{12}	4×10^{12}	4×10^{12}
Bunches/sign	2	1	1
Beam Power MW	38	0.7	1.0
ε_N π mm-mrad	50	90	195
Bending Field T	9	9	
Circumference km	8	1.3	0.3
Ave. ring field B T	6	5	3.5
Effective turns	900	800	450
β^* mm	3	8	9
IP beam size μm	2.8	17	187
Chromaticity	2000-4000	40-80	
β_{max} km	200-400	10-20	1.5
Lumin. $cm^{-2}s^{-1}$	10^{35}	10^{33}	2×10^{31}

energy range of most of the heavy Higgs in the minimal SUSY model (if that is the correct theory).

Although muon colliders remain a promising complement, to e^+e^- and hadron colliders, much work is still needed, including demonstration of μ production and cooling, detector, and radiation.

DISCUSSION

The muon collider concept promises to extend the high energy frontier to an unprecedented domain, with center of mass energies of 3 TeV or beyond as its goal. Considerable effort has already gone into the conceptual design of muon colliders, but much R&D remains to be carried out. Of particular importance are production targetry and cooling tests. The Muon Collider Collaboration represents a dedicated effort to address those issues and pave the way for a future muon accelerator complex.

A full high energy muon collider may take considerable time to realize. However, intermediate steps in its direction are possible and could help facilitate the process. Employing an intense muon source to carry out forefront low energy research, such as the search for muon - number non - conservation, represents one interesting possibility. For example, the MECO proposal at BNL aims for 2×10^{-17} sensitivity in their search for coherent muon - electron conversion in the field of a nucleus. To reach that goal requires the production, capture and stopping of muon at an unprecedented $10^{11} \frac{\mu}{sec}$. If successful, such an effort would significantly advance the state of muon technology.

More ambitious ideas for utilizing high intensity muon sources are also being explored. Building a muon storage ring for the purpose of providing intense high energy neutrino beams is particularly exciting. Such neutrino factories could have their own world class research program, with neutrino oscillation studies as the primary focus. Indeed, if very high intensities, $\sim 10^{21} \frac{\nu}{year}$, are attained and nature has been kind in her neutrino mass and mixing parameters, one could envision a complete exploration of the 3×3 neutrino mixing matrix and even the detection of CP violation in the oscillation phenomena.

If a neutrino factory is successfully accomplished, it would provide a major advancement. Its ambitious goals would test essentially all aspects of the muon collider concept, muon production, collection, cooling and acceleration. Furthermore, if properly coordinated, the neutrino factory complex might be suitably expanded into the First Muon Collider, perhaps a Higgs factory with center of mass energy $\sim$ 100 GeV.

High intensity muon experiments, neutrino factories, and other intermediate steps toward the muon collider are extremely important. They will greatly expand our abilities and build confidence in the credibility of high energy muon colliders. Progress may be slower than many would prefer, but remember, Rome was not built in a day.

ACKNOWLEDGMENTS

The author appreciates NNN99's organizers interest and invitation to write this paper. Special thanks to Dr. Diwan for extending the time, and to Dr. Paige for assisting with the latex problems; that made the completion of this report possible. This document was assembled largely from NFMCC existing sources, which have been cited among the references. Thanks to those individuals who contributed graphics, information, and assistance.

REFERENCES

1. The Neutrino Factory and Muon Collider Collaboration (NFMCC) home page: http://www.cap.bnl.gov/mumu/
2. http://neutrino.kek.jp/~ melissa/K2K/K2K2./html http://www.awa.tohoku.ac.jp/html/KamLAND/
3. See, for example, sec. 3.4 of the MINOS Technical Design Report, http://www.hep.anl.gov/NDK/Hypertext/minos_tdr.html

4. http://www.cern.ch/NGS/ngs99.pdf
5. The MiniBooNE project: http://www.neutrino.lanl.gov/BooNE
6. The Oak Ridge Large ν Detector http://www.orau.org/orland/
7. *Search for $\nu_\mu \rightarrow \nu_e$ Oscillations at CERN PS*, http://chorus01.cern.ch/~pzucchel/loi/
8. A.C. Melissinos unpublished note (1960).
9. C.M. Ankenbrandt *et al.*, *Status of muon collider research and development and future plans*, Phys. Rev. ST Accel. Beams **2**, 081001 (1999), and refrences therein.
10. See e.g., [11, 9, 1, 12], and references therein
11. K.T. McDonald, ed. for the Neutrino Factory and Muon Collider Collaboration, physics/9911009, 6 Nov, 1999, and references therein; ibid, Private comm.
12. http://lyoninfo.in2p3.fr/nufact99/ R.B. Palmer, C. Johnson, E Keil, BNL-66971, E. Keil, private Comm, Montauk, 99.
13. R.B. Palmer, Draft Paramets of a Neutrino Factory, MUC0046.
14. S. Kahn, private Comm; B. Autin, private Comm.
15. C. Kim, Private Comm.: received info. in Microsoft Word document format for simulation of the target to linac. These were then processed to pdf and ps format some of which is included; J. Wurtele, Private Comm.
16. A. Garren, Private Comm.: Bowtie-lattice design, simulation with code SYNCH; some of the info received is included; D.Cline, Private Comm.
17. S. Geer, *Neutrino Oscillation Rates at a Neutrino Factory*, MUC0051 (Sep. 13, 1999);
18. E.g.: S.L. Glashow and L.M. Krauss, Phys. Lett. **B190**, 199 (1987); S.P. Mikheyev and A.Y. Smirnov, Phys. Lett. **B429**, 343 (1998);V. Barger and K. Whisnant, Phys. Rev. D **59**, 093007 (1999), hep-ph/9812273; M. Maris and S.T. Petcov, Phys. Lett. **B457**, 319 (1999);
V. Berezinsky, G. Fiorentini, and M. Lissia, hep-ph/9904225; S. Goswami, D. Majumdar, and A. Raychaudhuri, hep-ph/9909453.
19. G.S. Vidaykin *et al.*, JETP Lett. **59**, 390 (1994);
B. Achkar *et al.*, Nucl. Phys. **B434**, 503 (1995).
20. E.g.: A. Zee, Phys. Lett. **B93**, 389 (1980); V. Barger, P. Langacker, J. Leveille, and S. Pakvasa, Phys. Rev. Lett. **45**, 692 (1980); V. Barger, S. Pakvasa, T.J. Weiler, and K. Whisnant, Phys. Rev. D **58**, 093016 (1998); S.M. Bilenky, G. Giunti, hep-ph/9905246.
21. Z. Maki, M. Nakagawa, and S. Sakata, Prog. Theor. Phys. **28**, 970 (1962). M. Nakagawa, hep-ph/9811358.
22. http://www.hep.anl.gov/ndk/hypertext/chooz.html
23. L. Wolfenstein, Phys. Rev. D **17**, 2369 (1978); S.P. Mikheyev and A.Y. Smirnov, Sov. J. Nuc. Phys. **42**, 913 (1986).
24. N. Hata and P. Langacker, Phys. Rev. D **56**, 6107 (1997), J.N Bahcall, P.I. Krastev, and A.Y. Smirnov, Phys. Rev. D **58**, 096016 (1998), J.N. Bahcall, P. Langacker, J. Bahcall and P. Krastev, Phys. Lett. **B436**, 243 (1998), hep-ph/9807525.
25. S. Geer, Phys. Rev. D **57**, 6989 (1998), hep-ph/9712290; A. Buena, M. Campanelli, and A. Rubbia, hep-ph /9808485; and hep-ph/9811390; http://fnalpubs.fnal.gov/archive/1999 hep-ph/9905420; V. Barger, S. Geer, and K. Whisnant, hep-ph/9906487; O. Yasuda, hep-ph/9910428;
I. Mocioiu and R. Shrock, hep-ph/9910554.
26. M. Tanimoto, Prog. Theor. Phys. **97**, 9091 (1997),J. Arafune, M. Koike, and J. Sato, Phys. Rev. D **56**, 3093 (1997),S.M. Bilenky, C. Giunti, and W. Grimus, hep-ph/9705300; H. Minakata and H. Nunokawa, Phys. Lett. **B413**, 369 (1997),H. Minakata and H. Nunokawa, *CP Violating vs. Matter Effect in Long-Baseline Neutrino Oscillation Phys. Rev. D* **57**, *4403 (1998),S.M. Bilenky, C. Giunti, and W. Grimus, Phys. Rev. D* **58**, *033001 (1998), M. Tanimoto, hep-ph/9906375; K.R. Schubert, hep-ph/9902215; K. Dick, M. Freund, M. Lindner, and A. Romanino, hep-ph/9903308; J. Bernabeu, hep-ph/9904474;M. Tanimoto, hep-ph/9906516; A. Donini, M.B. Gavela, P. Hernandez, and S. Rigolin, hep-ph/9909254;H. Fritzsch and Z.-Z. Xiang, hep-ph/9909304;A. Romanino, hep-ph/9909425; M. Koike and J. Sato, hep-ph/9909469; J. Sato, hep-ph/9910442. hep-ph/9910442.*
27. *A. Blondel, http://alephwww.cern.ch/~bdl/muon/nufacpol.ps*
28. *V. Barger, Y.-B. Dai, K. Whisnant and B.-L. Young, Phys. Rev. D* **59**, *113010 (1999), hep-ph/9901388;A. Kalliomaki, J. Mallampi, and M. Tanimoto, hep-ph/9909301;A. Donini, M.B. Gavela, P. Hernandez, and S. Rigolin, hep-ph/9910516.*
29. *See, for example, B.J. King, AIP Conf. Proc.* **435**, *334 (1998). D.A. Harris and K.S. McFarland, ibid. p. 505;*
30. *D. B. Cline (ed.),* Physics Potential and Development of $\mu^+\mu^-$ Colliders *AIP Conf. Proc.* **352** *(1996).*
31. *The $\mu^+\mu^-$ Collider Collaboration,* $\mu^+\mu^-$ Collider Feasibility Study, *BNL-52503, FERMILAB-Conf-96/092, LBNL-38946 (July 1996); http://www.cap.bnl.gov/mumu/book.html*
32. *Z. Parsa, ed., Future High Energy Colliders, AIP CP* **397**, *AIP-Press, Woodbury, NY (1997).*
33. *Z. Parsa, Ionization cooling and Muon Dynamics, AIP CP 441, 289-294 (1997).*
34. *Z. Parsa, New High Intensity Muon sources and Flavor Changing Neutral Currents, World scientific Publishing, pp 147-153 (1998).*
35. *Z. Parsa, ed., Beam Stability and Nonlinear Dynamics, AIP CP 405 AIP-Press, Woodbury, NY (1997).*
36. *Z. Parsa, Lasers and Future High Energy Collliders, STS-Press, pp 823-830 (1997).*
37. *Kamal, B., Marciano, W., Parsa, Z.. Resonant Higgs enhancement at the first muon collider, AIP CP 441, pp174- (1997); ibid, AIP 435 pp567-662 (1997).*
38. *Z. Parsa, Polarization and Luminosity requirements for the First Muon Collider, Procd. of AAC98, AIP-Press, NY.(1998).*
39. *Z. Parsa, Polarization Effects at a Muon Collider,* Presentation at EPAC98, Stokholm, Sweeden, June 1998.
40. *Z. Parsa, Muon Dynamics and Ionization Cooling at Muon Colliders, Procd. of EPAC98, Stockholm, Sweden, Vol 2, pp.1055-.*
41. *C.N. Ankenbrandt et al., Ionization Cooling Research and Development Program for a High Luminosity Muon Collider, FNAL-P904 (April 15, 1998), http://www.fnal.gov/projects/muon_collider/*
42. *Neutrino Factory Feasibility Studies at Fermilab: http://www.fnal.gov/projects/muon_collider/nu_factory/*
43. *N. Mokhov, Carbon and Mercury Targets in 20-T Solenoid with Matching,* MUC0061; ibid, private comm. V. Balbekov, Private Comm.
44. Experiment E-910 at BNL-AGS; http://www.nevis.columbia.edu/heavyion/e910/